Electrical Power and Energy Systems 157 (2024) 109796

Contents lists available at ScienceDirect

International Journal of Electrical Power and Energy Systems

journal homepage: www.elsevier.com/locate/ijepes

Reconfiguration of 123-bus unbalanced power distribution network analysis by considering minimization of current & voltage unbalanced indexes and power loss

Nisa Nacar Cikan [a,*], Murat Cikan [b]

[a] Electrical and Electronics Engineering Department, Cukurova University, 01330, Adana, Türkiye
[b] Adana Organize Industrial Region of Vocational School Technical Sciences, Cukurova University, Adana 01410, Türkiye

ARTICLE INFO

Keywords:
Reconfiguration
Voltage and Current Unbalance Index
123-Bus Unbalanced Power Distribution Test System
Slime Mould Algorithm
OpenDSS

ABSTRACT

Reconfiguration is an efficient solution for loss minimization and system improvement in the power distribution network (PDN). Although reconfiguration has been studied for a long time, most works to date approach the problem considering the system balanced with constant PQ-load, while real PDNs are unbalanced due to uneven loads. On the other hand, unbalanced loadings can lead to increased energy losses, violate capacity limits, and affect power quality, resulting in voltage and current unbalance (CVU). Therefore, methods that mitigate the adverse effects of CVU are necessary. In this paper, the slime mould algorithm (SMA) is used to solve the reconfiguration problem (RecPrb) in a 123-bus unbalanced system with the objectives of minimization of power loss, the current unbalance index (CUI), and voltage unbalance index (VUI). The system is evaluated in two parts by considering many cases where power losses and unbalanced indexes are gradually minimized with the presented scenarios. A three-phase unbalanced backward-forward-load-flow Matlab script is written, and all simulations are run in the Matlab environment. The test system is built in OpenDSS and Matlab/Simulink to verify the script's correctness, and the obtained results are also validated with the IEEE-PES data. The effectiveness of the SMA method is further assessed by comparing it with well-known EO and DE algorithms using over 15 statistical methods to find the most efficient algorithm that solves the RecPrbs of unbalanced test systems. The results demonstrate the robustness and efficiency of the SMA method in minimizing losses, limiting unbalanced indexes, and improving the system's voltage profile.

1. Introduction

The distribution system is essential to the power network linking electricity customers and utilities. The network operators aim to provide electricity to their customers economically and in a reliable way with minimum power loss. The increasing load demand of power network users complicates the system's operation, overloads the distribution feeders, and, most importantly, increases the system losses. Power loss minimization is one typical and primary objective considered in power distribution network (PDN) planning. The network reconfiguration minimizes losses to improve the overall system performance and relieves PDN overloads as operating conditions change to balance the loads [1]. Reconfiguration in PDN modifies the network's topological structure by altering the open/close positions of tie switches (TSs) and sectionalizing switches (SSs). Throughout the last two decades, numerous approaches have been used to solve network reconfiguration problems (RecPrbs) [2]. These approaches can be broadly categorized as smart search methods and traditional techniques (deterministic) that apply linear/nonlinear methods [3]. Deterministic methods are frequently unsuccessful in obtaining the global optima for large-scale nonlinear or non-convex problems that are hard to differentiate and get caught up in the local optima [4]. Thus, metaheuristic techniques have emerged as an alternative to solving RecPrbs. Metaheuristic approaches provide appropriate solutions by converging quickly and might require fewer calculations [2].

Numerous papers are presented in the literature that has comprehensively discussed the RecPrbs using various optimization techniques. In [2,5], previous research works to solve RecPrbs were reviewed and summarized. Although reconfiguration of PDN has been studied for a long period of time, most of the works to date have treated the distribution networks as balanced PDN when the taxonomy of the reviewed

* Corresponding author.
E-mail address: ncikan@cu.edu.tr (N. Nacar Cikan).

https://doi.org/10.1016/j.ijepes.2024.109796
Received 11 December 2022; Received in revised form 18 November 2023; Accepted 21 December 2023
Available online 24 January 2024

Nomenclature

Abbreviation

CUI	current unbalance index
CVU	current & voltage unbalance
DE	differential evaluation algorithm
DG	distributed generation
EO	equilibrium optimizer algorithm
OpenDSS	electric power distribution system simulator
PDN	power distribution network
PDNR	power distribution network reconfiguration
IEEE-PES	IEEE power and energy society
RecPrbs	reconfiguration problems
SMA	slime mould algorithm
SSs	sectionalizing switches
TSs	tie-switches
UPDN	multi-phase unbalanced power distribution network
VUI	voltage unbalance index
WMC	written Matlab code

SMA Parameters and Symbols

a	is a function of iteration and maximum iteration number
DF	obtained best fitness cost in all iterations
Fit_{Best}, Fit_{Worst}	determined best and worst fitness value in the current iteration, respectively
iter	iteration number
max_{iter}	maximum iteration number
r	random value between [0,1]
S(i)	shows the fitness of $\vec{X}$
Up_B, Lo_B	search space of upper and lower boundaries
$\vec{v}_b$, $\vec{v}_c$	oscillates between [-a, a] and [-1, 1]
$\vec{W}$	control weight parameter
$\vec{X}$	slime mould position
$\vec{X_A}$, $\vec{X_B}$	randomly selected slime moulds
$\vec{X}_b$	best location found so far
z	constant value and is chosen 0.03.

Parameters Symbols

E	edges
$e_1, e_2, \ldots, e_m$	edge set (edges)
e_j	vertex j of graph G
$\|E(G)\|$	number of edges (branches, size)
F	fuse
G	a connected graph
G(V, E)	is a collection of vertices (V) and edges (E)
I_i	current flow at line i
I_i^{max}	maximum current at line i
L	load
m	number of edges (branches)
n	number of vertices (bus, nodes)
N_{Branch}	number of branches
N_{Bus}	number of buses
N_{Gen}	number of generators
N_{Load}	number of loads
$P_{i,Gen}^{abc}$	supplied active power by generator i
P_i^{max}	maximum active power at bus i
$P_{i,loss}^{abc}$	active power loss
$P_{i,Load}^{abc}$	demand load power at bus i
$Q_{i,cap}^{min}, Q_{i,cap}^{max}$	minimum and maximum capacity of capacitor bank i, respectively
Q_i^{max}	maximum reactive power at bus i
Q(G)	incidence matrix
$r_{(i)}$	line resistance at branch i
S	switch
Suppliers	number of suppliers (feeder)
$S_{i,\,line}^{max}$	maximum power flow at line i
Sw	binary variable (’1′ or ’0′)
Tap_i^{min}, Tap_i^{max}	minimum and maximum voltage regulator tap position limits, respectively
V	vertices
$v_1, v_2, \ldots, v_n$	vertex set (vertices)
V_i	voltage magnitude at bus i
V_i^{feeder}	voltage magnitude at feeder i
V_i^{min}, V_i^{max}	lower and upper voltage of bus i, respectively.
$V_{i,Tap}^{min}, V_{i,Tap}^{max}$	minimum and maximum voltage regulator voltage, respectively
|V(G)|	number of vertices (buses, order).
X_E, X_A	expected and actual values, respectively
$Xtrf_i^{min}, Xtrf_i^{max}$	minimum and maximum transformer operation limits, respectively
$X_k^{Neg,\ seq}, X_k^{Pos,\ seq}$	negative and positive sequence of voltage/current, respectively
∧	number of tie-switches

works is carefully examined. The balanced modeling initially approaches the unbalanced system as a balanced one. Next, it derives either the decoupled three single-phase network or a positive sequence system [6]. Recently, in [3], comprehensive research has been conducted by statistically comparing the performance of 11 popular metaheuristic algorithms in reducing power losses and improving the system’s reliability. The algorithms are tested in four different balanced test systems. In [7–9], reconfiguration with distributed generator (DG) allocation was presented using various algorithms based on balanced test systems. On the other hand, in practice, PDN is inherently unbalanced due to the varied load demands and untransposed and mutually coupled lines. Multi-phase unbalanced power distribution network (UPDN) examination provides more accurate system control and analysis.

Most works based on unbalanced three-phase PDN to solve the network RecPrbs are focused on small-scale test systems such as 19-bus, 25-bus, and so on. In [10], reconfiguration of unbalanced 33-bus &69-bus test systems was proposed to minimize power loss, voltage unbalance index (VUI), and energy not supplied index (ENS). An improved Corona-virus Herd Immunity Optimizer (ICHIOA) algorithm was used, and the performance of the presented algorithm was compared with some other algorithms. In [11], a 24-h period of reconfiguration model as mixed-integer linear programming (MILP) was shown for a 34-bus unbalanced test system. In [12], the Firefly algorithm based on a fuzzy domain was proposed to minimize losses and bus voltage deviation. The proposed approach was applied to 19-bus and 25-bus unbalanced PDN. In [13], the reinforcement learning (RL) technique was used to formulate the RecPrb, and the presented approach was applied to the unbalanced 34-bus and 13-bus test systems. A few studies have been published based on three-phase unbalanced networks, such as the 123-bus test system, due to their high complexity and difficulty analyzing. Thus, further studies are needed to address complex networks with load imbalances. The pros and cons of research papers in literature to solve the RecPrb in 123-bus UPDN are reviewed as follows: In [14], a deep-learning-based robust method was applied to solve the RecPrb. The approach was mainly focused on the uncertainties (by placing distributed generators) in the PDN and only evaluated cost. In [15], the reconfiguration technique was developed for normal and post-fault

conditions. Three loading cases were considered, such as the light load level is half the nominal load and the heavy load is 1.5 times the nominal load, respectively. However, these operating conditions did not affect reconfiguration (switch status) due to the linear increase and decrease in the loadings. The same switches (4 and 6) were opened in all conditions. In [16], a modified backward-forward (BF) sweep-based power flow method was presented to solve the RecPrb, and the technique was tested on 123-bus and 13-bus test systems. Some tie switches were added to modify the test systems and increase the complexity. However, the 123-bus test system's obtained power loss value was approximately double the nominal power loss compared to IEEE-PES data. In [17], dynamic reconfiguration was performed using a selective bat algorithm (SBAT). In [18], the dynamic reconfiguration model coupled with the uncertainty of DG units was proposed. The 123-bus test system was only briefly evaluated in terms of cost. In [19], reconfiguration was performed, considering the reliability and power loss. In [14,15,17–19], the modified 123-bus test system was examined by removing equipment like voltage regulators, transformers, and capacitor banks. Removing all the equipment simplifies the test system; however, it might not provide realistic results.

In practice, the unbalanced loadings at the buses increase energy losses. Losses violate the capacity limit and cause power quality deterioration [12]. The current & voltage unbalance (CVU) are critical power quality problems that are highly harmful to PDN and the equipment connected to the system [20,21]. The system's inherent characteristics, such as unequal distribution of single-phase and two-phase loads between three-phase lines, plus the equipment disturbances in the system, are the main reasons for CVU [20,21]. High CVU can cause malfunctioning, failure of protection devices, overheating, and reduced functional equipment [21]. Therefore, it is necessary to develop methods that reduce the effects of CVU. The true definition of measuring voltage unbalance metric is presented by the IEEE as voltage unbalance index (VUI) [22]. The other metric to measure current unbalance is the current unbalance index (CUI) [21]. There are different standards to limit VUI; however, the limits of CUI are still unclear [20]. DGs allocation is the one way to minimize VUI and has been discussed in some research works. On the other hand, the CUI is another parameter that affects the system's power quality that has not been addressed and analyzed deeply so far. Especially electrical machines (frequently used in DG implementation) are harmed by the current imbalance [21]. In [21], VUI and CUI were limited simultaneously for the first time by optimizing the sizes of capacitors using iterated local search (ILS) algorithm. In [23], the VUI and CUI values were determined at the feeder bus after DG allocation. Few studies have been conducted to solve the RecPrb in UPDN by considering the effects of VUI and CUI values. In [24], the RecPrb in PDN was solved by considering the direct impacts of VUI and CUI on unbalanced 19-bus and 25-bus test systems. Additionally, the modified 123-bus test system was tested by removing equipment like voltage regulators, capacitor banks, etc. Removing all the equipment simplifies the test system; however, it might not provide realistic results. No detailed information was provided for the 123-bus test system, such as the effects of unbalanced indexes before/after reconfiguration, and the considered objective function was power loss. In literature, it is noticed that finding a feasible solution by considering CUI is complicated, and thus further studies are needed to assess its impact on PDN.

This paper aims to fill the literature gaps elaborately explained above. The contribution of this study is as follows.

- An unbalanced 123-bus test system has been presented comprehensively and analyzed in detail to solve the RecPrb in UPDN by considering power loss and unbalanced indexes as objective functions.
- Two different scenarios with many cases are presented to increase the system complexity of the system and make a comparison among them.
- In particular, the effects of CUI on the test system and the relation with power loss are analyzed and demonstrated.
- Slime mould algorithm (SMA) [25] is used to solve the RecPrb of a 123-bus UPDN to minimize losses, unbalance indexes and improve the voltage profile. The results of the method are compared with the well-known Equilibrium Optimizer (EO) [26] and Differential Evaluation (DE) [27] algorithms by using more than 15 statistical methods to find the most efficient algorithm that solves the RecPrbs of 123-bus UPDN.
- Unlike the literature, all equipment, such as capacitor tanks, transformers, and voltage regulators, are not removed from the 123-bus test system to obtain realistic results.
- A Matlab script is written, and all scenarios with different cases are executed in the Matlab environment. Moreover, the unbalanced test system is also set up in OpenDSS and Matlab/Simulink to verify and guarantee the correctness of written Matlab code (WMC). The obtained results from three distinct platforms are also compared with IEEE-PES data. Comparing and validating the results in four different platforms provides a reliable and decisive advantage in successfully solving RecPrbs in large-scale test systems.

The structure of this paper is as follows: Section 2 presents the RecPrb in PDN and the mathematical model of the problem. Section 3 introduces the SMA method, Section 4 presents the IEEE 123-bus UPDN and the comparison of results of four different platforms considering the initial case, Section 5 presents the results and discusses the test system in many aspects, and finally, Section 6 highlights the conclusions.

2. Reconfiguration of power distribution network

Line losses in electrical power systems account for 5 to 15 % of the transmitted power [3]. In this regard, loss minimization is necessary for the system's economic operation. One of the main objectives of the power distribution network reconfiguration (PDNR) is minimizing power loss. Moreover, maintaining the bus voltages at nominal levels helps the system's optimum operation. The other important objective of UPDN is to operate the system in a reliable way by minimizing the current and voltage unbalance indexes. In the present study, the RecPrb in UPDN is solved by minimizing active power losses, CUI &VUI, and improving the bus voltage magnitude considering certain constraints. This study's objective functions and constraints are presented in subsections.

2.1. Radiality

The goal is to maintain the radial structure of the PDN after changing the switch positions. Radial networks are commonly employed as these structures are simple to operate, design, and easy to locate protective devices [28]. The power flows unidirectionally from the substation downstream to the consumers in a radial network, as shown in Fig. 1. Graph theory is used to preserve the radial form of the PDN after reconfiguration. In a unidirectional graph, let G(V,E) be a graph with $V(G) = (v_1, v_2, \ldots, v_n)$ and $E(G) = (e_1, e_2, \ldots, e_m)$. Here, |V(G)| (n) and |E(G)| (m) show the number of vertices and edges, respectively.

Lemma 1. *If $m > n - 1$, then G has a loop.*

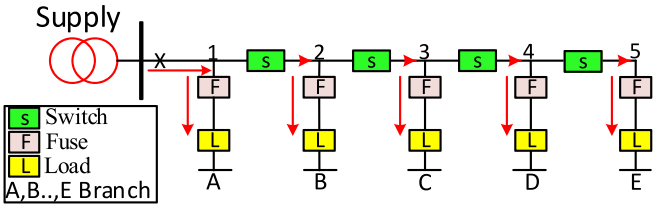

Fig. 1. 6-Bus radial power distribution network.

Lemma 2. *If $m < n-1$, then G is not connected.*

Theorem 1. *Assuming G is a connected graph using n vertices, rank Q(G) = n − 1*[29]*. Q(G) is defined in Eq. (1).*

$$Q(G) = \begin{cases} 0 & \text{if vertex i and edge } e_j \text{ are not incident} \\ -1 & \text{if vertex i is the negative end of } e_j \\ 1 & \text{if vertex i is the positive end of } e_j \end{cases} \quad (1)$$

Lemma 3. *Columns $j_1, \ldots, j_k$ of Q(G) are linearly independent if and only if the corresponding edges of G cause an acyclic graph* [29].

Theorem 2. *A graph G is a tree if and only if, G is:*

- acyclic and |E(G)|= |V(G)|-1
- a connected graph and acyclic (without cycles)
- a connected graph and |E(G)|= |V(G)|-1

At least two of these three properties (in theorem 2) provide the necessary and sufficient conditions for ensuring the tree structure. As explained in Theorem 2, a tree can be defined as a connected graph without a loop. If the graph model is adapted to PDN, |E(G)| demonstrates the number of the branch (N_{Branch}) and |V(G)| shows the number of the bus (N_{Bus}). The obtained equations are given below by using Theorem1 and Theorem2.

$$N_{Branch} = N_{Bus} - 1 \quad (2)$$

$$\text{rank}(Q(G)) = N_{Bus} \quad (3)$$

If the PDN meets the conditions in Eqs (2) and (3), then the power network operates in radial topology. In addition, the following prerequisites must be satisfied.

- Every bus is within the subgraph [30].
- Every load has a single supply source [2].
- Each bus in the system should be connected to a substation [3].

In Eq. (4),'∧' denotes the number of TSs to preserve the radial form of the UPDN.

$$\wedge = N_{Branch} - N_{Bus} + \text{Suppliers} \quad (4)$$

where Suppliers, N_{Bus}, and N_{Branch} denote the number of feeders, buses, and branches, respectively.

2.2. Constraints

The variations in voltage should be within the defined limits, as shown in Eq. (5.a). The range for the bus voltage and the feeder voltage should be ± 10 % (Eq. (5. b)), and ± 5 % (Eq. (5.c)), respectively.

$$V_i^{min} \le V_i \le V_i^{max} \quad (5a)$$

$$0.9.V_i \le V_i \le 1.1.V_i \quad (5b)$$

$$0.95.V_i^{feeder} \le V_i^{feeder} \le 1.05.V_i^{feeder} \quad (5c)$$

The maximum current limit is given in Eq. (6).

$$I_i \le I_i^{max} \quad (6)$$

Limits for Voltage Regulator Tap Position are presented in Eq. (7)

$$\begin{aligned} Tap_i^{min} &\le Tap_i \le Tap_i^{max} \\ V_{i,Tap}^{min} &\le V_{i,Tap} \le V_{i,Tap}^{max} \end{aligned} \quad (7)$$

Power Balance Equation is shown in Eq. (8).

$$\sum_{i=1,}^{N_{Gen}} P_{i,Gen}^{abc} = \sum_{i=1,}^{N_{Load}} P_{i,Load}^{abc} + \sum_{i=1,}^{N_{Branch}} P_{i,Loss}^{abc} \quad (8)$$

Capacitor Tanks limit is shown in Eq. (9)

$$Q_{i,cap}^{min} < Q_{i,cap} < Q_{i,cap}^{max} \quad (9)$$

Transformer operation limit is given in Eq. (10)

$$Xtrf_i^{min} < Xtrf_i < Xtrf_i^{max} \quad (10)$$

Constraint for Line Flow Security is presented in Eq. (11)

$$S_{i,line} < S_{i,line}^{max} \quad (11)$$

Constraint for System Radiality is shown in Eq. (12)

$$\begin{aligned} &rank(Q(G)) = N_{Bus} - 1 \\ \wedge &= N_{Branch} - N_{bus} + Suppliers \end{aligned} \quad (12)$$

Constraint for Power Source Limit is given in Eq. (13)

The total loads of a certain partial network cannot exceed the capacity limit of the corresponding power source

$$P_i \le P_i^{max} \quad (13)$$

2.3. Power loss as an objective function

The purpose is to minimize losses in the system by maintaining the bus voltages at a specific range. Thus, Eq. (14) is used to calculate active power loss.

$$P_{loss}(i, i+1) = r_i.|I_i|^2 \quad (14)$$

The total power loss is calculated by summing the losses at branches as defined in Eq. (15).

$$P_{Loss}^{min} = \sum_{i=1,}^{N_{branch}} r_{(i)} \cdot \left(\frac{P_i^2 + Q_i^2}{V_i^2} \right) .Sw_{(i)} \quad (15)$$

where r indicates the branch resistance, Q_i, P_i and V_i denote reactive power, active power, and bus voltage, respectively. N_{branch} indicates the number of branches, and Sw represents whether or not the branch is energized (active). The Sw value is '1′ when the branch is active; otherwise, it has a value of '0′.

2.4. Unbalance indexes as objective functions

The literature and electric distribution market indicate that the unbalance index's true definition could be determined through the percentage ratio of the negative sequence to the positive sequence component. Thus, the description is adapted in this paper as in Eq. (16). A comprehensive examination of the subject can be found in [21,22].

$$\%\,Unb_{Index} = \frac{\left|X_k^{Neg,\ seq}\right|}{\left|X_k^{Pos,\ seq}\right|}.100 \quad (16)$$

The flowchart of the applied method used in PDNR problem is shown in Fig. 2.

3. Slime mould algorithm (SMA)

SMA is a population-based metaheuristic algorithm motivated by the oscillation mode of slime mould, which are simple organisms capable of solving complex optimization problems [25]. SMA works by imitating slime mould's morphological and behavioral changes while foraging. The basic idea behind the SMA is to simulate the behavior of slime molds as they forage for food in their environment. Slime molds are known for

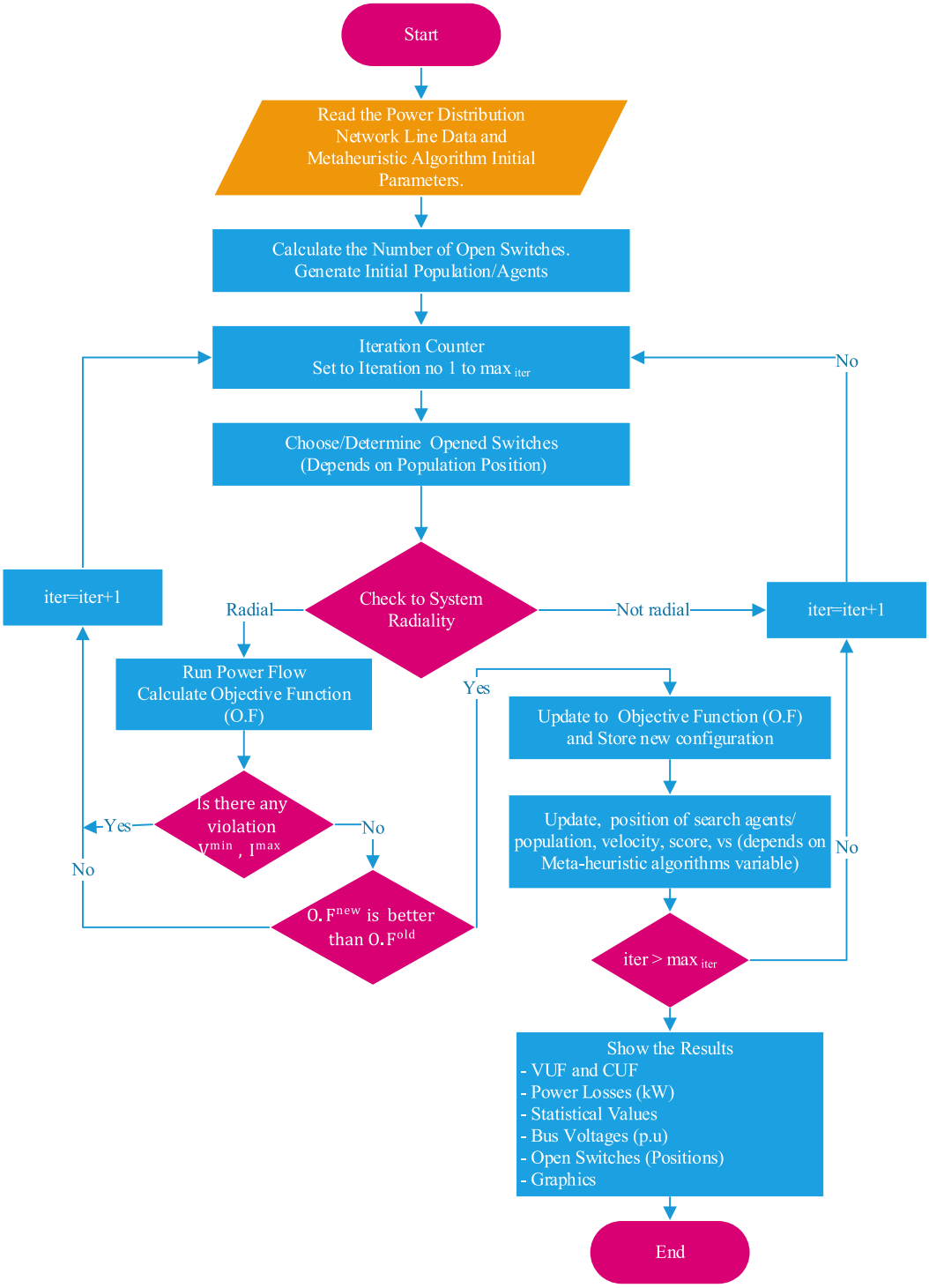

Fig. 2. Flowchart of the applied method used in PDNR problem.

their ability to explore their surroundings and find the most efficient path to their target by leaving a trail of pheromones that attracts other members of the colony. In SMA, a population of virtual slime molds is created, and each slime mold is represented by a point in a multi-dimensional solution space.

The slime molds in SMA move in the solution space based on simple rules, such as moving towards areas with higher pheromone concentrations, avoiding obstacles, and exploring new areas. Slime molds can also communicate and share information with their neighbors, allowing for cooperative behavior. As the simulation progresses, the slime molds iteratively update their positions and pheromone concentrations based on the fitness of their current solutions. Over time, the slime molds converge towards an optimal solution, guided by the pheromone trails left by their peers. It tries to find quality food sources equivalent to seeking optimal solutions for slime moulds.

SMA has been successfully applied to various optimization problems, including vehicle routing, scheduling, image processing, and supply chain management. One of the key advantages of SMA is its ability to find near-optimal solutions in complex and dynamic environments, as it is capable of adapting to changing conditions through local interactions

and global information sharing among the slime molds. However, like other metaheuristic algorithms, SMA also has limitations, such as the need for careful parameter tuning and the possibility of getting trapped in local optima. Nonetheless, SMA continues to be an active area of research and shows promise in solving a wide range of optimization problems. The SMA's general logic comprises three primary elements: searching food, approaching food and enveloping food as demonstrated in Fig. 3.

The slime mould can proceed toward food depending on the odor in the air. In order to represent this behavior mathematically, the following Eq. (17) to Eq. (20) have been suggested to simulate the contraction mode.

$$\vec{X}^{t+1} = \begin{cases} \vec{X}_b^{(t)} + \vec{v}_b.\left(\vec{W}.\vec{X}_A^{(t)} - \vec{X}_B^{(t)}\right) & r < p \\ \vec{v}_c.\vec{X}^{(t)} & r \geq p \end{cases} \tag{17}$$

where $\vec{v}_b$ and $\vec{v}_c$ oscillates between [-a, a] and [-1, 1], respectively. The formulas for 'a' and 'p' parameters are presented in Eq. (18). $\vec{X}_b$ Indicates the best location found so far, $\vec{X}_A$ and $\vec{X}_B$ are randomly selected slime moulds,

$$p = \tanh|S(i) - DF| \tag{18}$$

$\vec{W}$ denotes the control weight parameter. The formula of $\vec{W}$ is given in Eq. (19).

$$\vec{W} = \begin{cases} 1 + r.\log_{10}\left(\frac{Fit_{Best} - S(i)}{Fit_{Best} - Fit_{worst} + \epsilon} + 1\right) & \text{, condition} \\ 1 - r.\log_{10}\left(\frac{Fit_{Best} - S(i)}{Fit_{Best} - Fit_{worst} + \epsilon} + 1\right) & \text{, others} \end{cases} \tag{19}$$

ϵ avoids to denominator is zero ($Fit_{Best} = Fit_{worst}$). The slime mould updates its location depending on the food concentration. The region's weight gets more significant when the food concentration is enough and smaller when the food concentration is limited, respectively. Based on this principle, the formula of the slime mould for updating its location is given in Eq. (20).

$$\vec{X}^{t+1} = \begin{cases} \vec{X}_b^{(t)} + \vec{v}_b.\left(\vec{W}.\vec{X}_A^{(t)} - \vec{X}_B^{(t)}\right) & r < p \\ \vec{v}_c.\vec{X}^{(t)} & r \geq p \\ rand(Up_B - Lo_B) + Lo_B & rand(.) < z \end{cases} \tag{20}$$

Up_B, and Lo_B indicate the search ranges' upper and lower boundaries, respectively. 'r' represents the random value in [0,1]. A biological oscillator produces the propagation waves by tending to be in a quality food concentration position.

4. IEEE 123-bus unbalanced distribution test system

The methodology is applied to the IEEE 123-bus test system shown in Fig. 4. The IEEE 123-bus test feeder is notable for its various features, which are extensively explained in [31]. The test system is characterized by a number of distinctive attributes that distinguish it from other test feeders. The total reactive power, active power, and nominal voltage in the test system are 1920 kVar, 3490 kW, and 4.16 kV, respectively. In the initial case, the total active and reactive power losses were stated in [31] as 95.611 kW and 193.727 kVar, respectively.

The 123-bus multi-phase UPDN comprises features as follows:

- Four shunt capacitor banks, three of which are connected to single-phase buses (88, 90, and 92), while the remaining one is connected to a three-phase bus (83).
- Four step-voltage regulators, connected in a wye (Y) configuration: On-Rgltr-1 (150,149) on all three phases, On-Rgltr-2 on single-phase A (9–14), On-Rgltr-3 on phases A-C (25,26), and On-Rgltr-4 on all three phases (160,67).
- A delta-delta transformer with a rating of 150 kVA and a line-to-line voltage ratio of 4.16 kV/0.48 kV is located at edge (61, 610) of the distribution network.
- Unbalanced spot loads (constant: Z, I, and PQ). These loads are connected in either a wye (Y) or delta (Δ) configuration. The IEEE 123-bus is a radial distribution network that exhibits considerable load imbalance owing to the inclusion of single-phase, two-phase, and three-phase loads. Fig. 4 depicts the network's one-line diagram, wherein 85-load-buses are identified by triangular-shaped cyan markers.
- Overhead (in 11 different configurations) and underground (in 1 configuration) line segments with multiple phases.
- The test system consists of 12 switches.

Table 1 shows the data on the switch statuses provided by IEEE-PES. The switches between nodes 54–94 and 151–300 are purposefully left open to protect the system's radial topology. These two switches can only ensure radiality. The other open switches (7,8, 11, and 12) have no impact on the system's radial structure because they are connected to buses at endpoints where no loads are connected.

As demonstrated in Fig. 4, all open switches (except 9 and 10 in Table 1) are closed to enlarge the search space and increase the system's

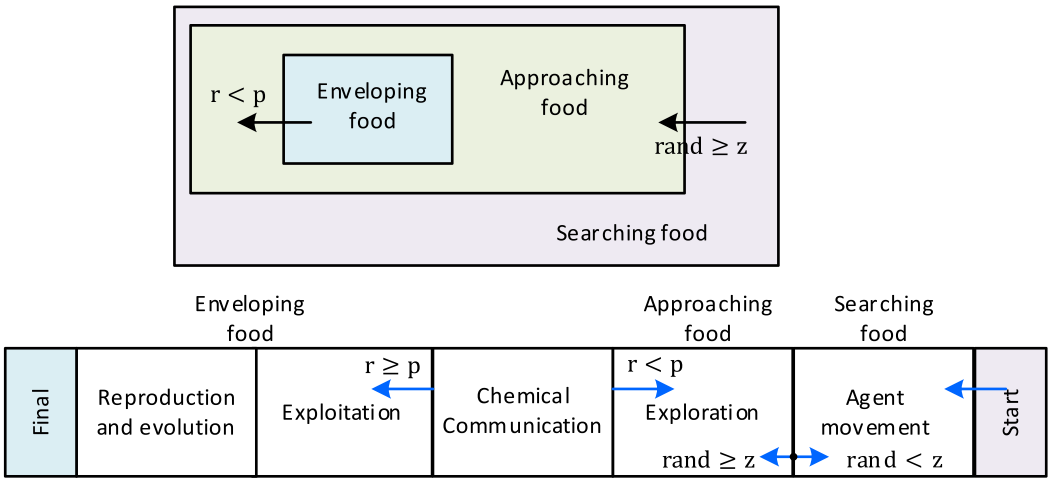

Fig. 3. Slime mould algorithm steps.

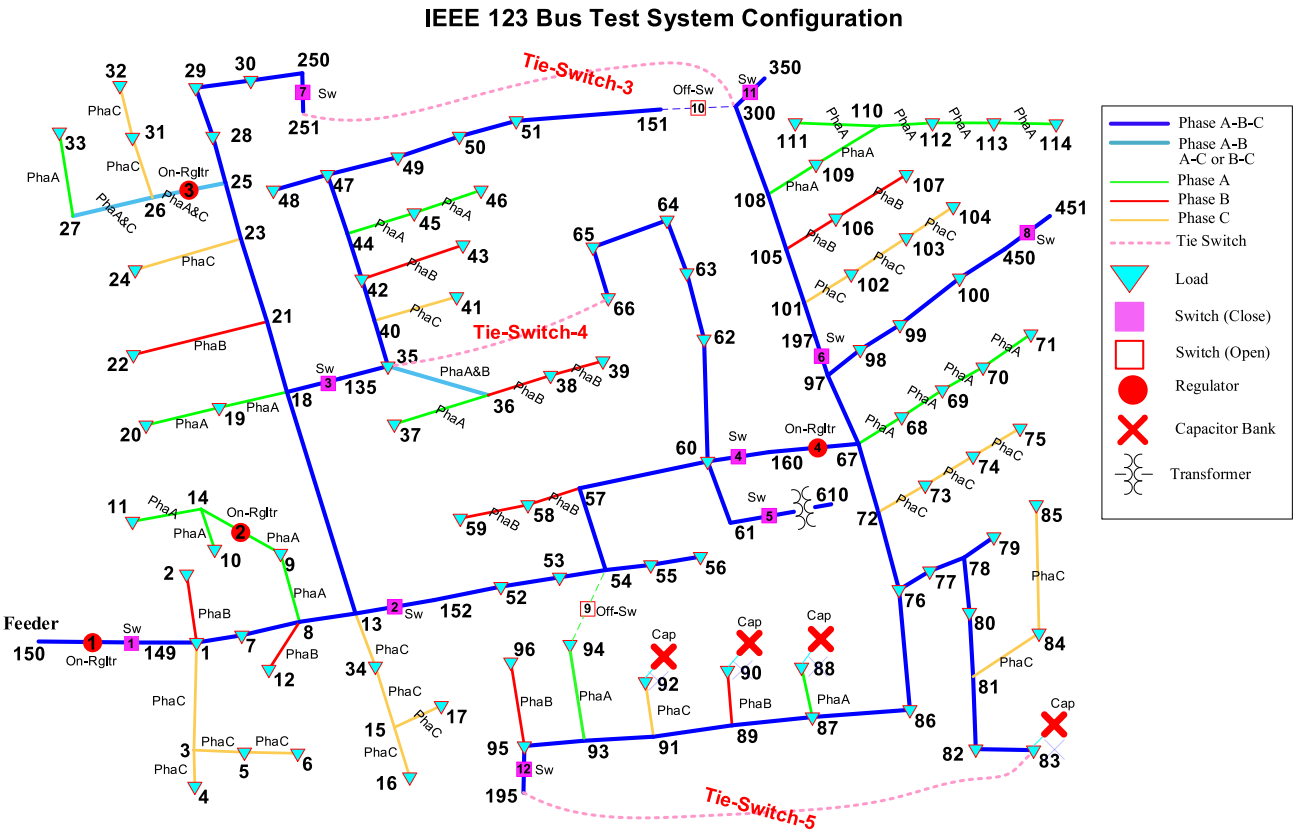

Fig. 4. IEEE-PES 123-bus UPDN test system.

Table 1
Initial case switch locations and statuses based on IEEE-PES 123-bus test system.

Switch No	1	2	3	4	5	6	7	8	9	10	11	12
From	13	18	60	61	97	150	250	450	**54**	**151**	300	95
To	152	135	160	610	197	149	251	451	**94**	**300**	350	195
Switch Status	Closed	Closed	Closed	Closed	Closed	Closed	Open/closed	Open/closed	**Open**	**Open**	Open/closed	Open/closed

complexity. There is a single switch on phase-A between buses 54 and 94, while all other pairs of buses with switches feature breakers on all three phases in the distribution network.

4.1. Initial case

The 123-bus UPDN comprises three-phase, two-phase, single-phase overhead, and three-phase underground line segments with unbalanced and balanced loads connected in wye (Y) or delta (Δ). This complexity makes the system rather challenging to analyze. Fig. 5 and Fig. 6 present the WMC and IEEE-PES data comparison results regarding relative errors (RE) of branch currents and bus voltage magnitudes.

Eq. (21) shows the relative error formula.

$$\delta = \left| \frac{X_A - X_E}{X_E} \right| \tag{21}$$

where, X_E and X_A are expected (IEEE-PES test case) and actual (calculated) values, respectively. The maximum and minimum current relative error for each phase $I^{abc}_{max} = [4.441, 5.1243, 4.8151].10^{-4}$ and is $I^{abc}_{min} = [1.335, 2.587, 3.638].10^{-7}$, respectively. The maximum and minimum voltage relative error for each phase is $V^{abc}_{max} = [5.076, 2.1957, 3.4796].10^{-4}$, and $V^{abc}_{min} = [1.79, 5.23, 4.05].10^{-7}$, respectively. Voltage and current magnitudes relative errors change between the minimum (10^{-7}) and maximum (10^{-4}), demonstrating that

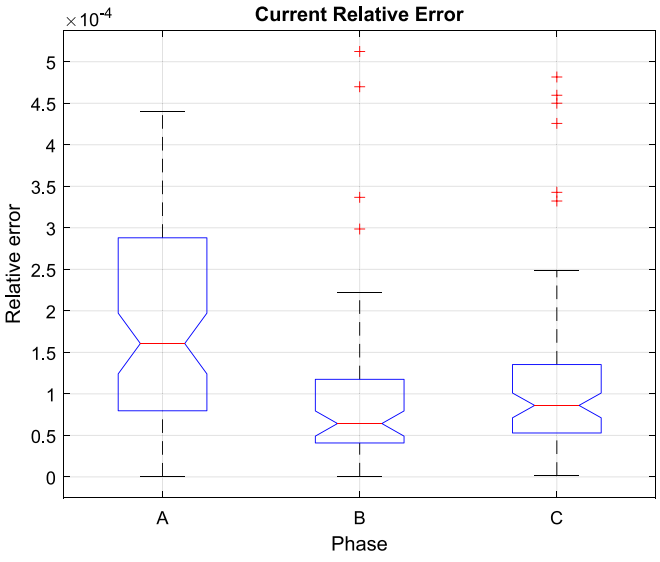

Fig. 5. Current RE of WMC and IEEE-PES.

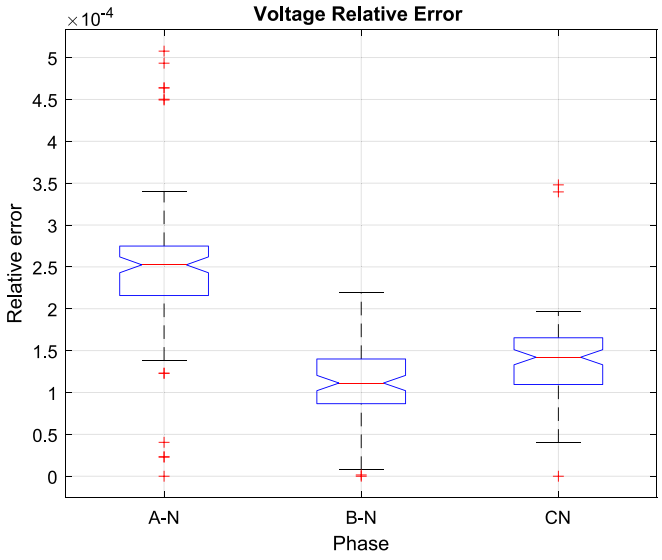

Fig. 6. Voltage RE of WMC and IEEE-PES.

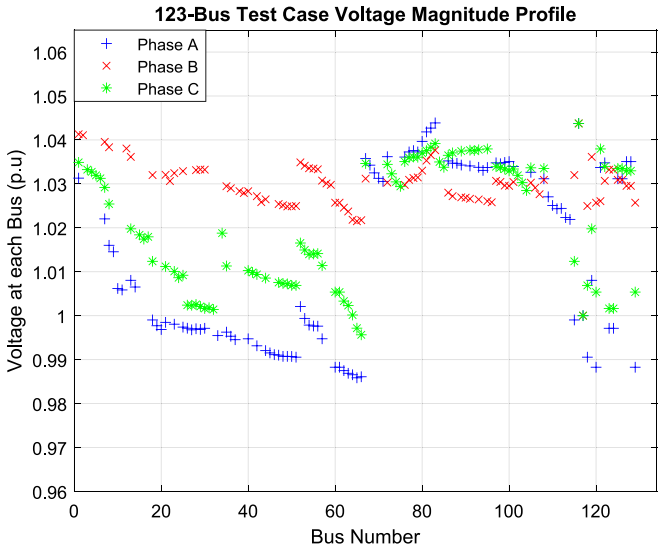

Fig. 7. Voltage profile of 123-bus UPDN.

the WMC aligns with the IEEE data findings. Fig. 7 shows the voltage profile for each phase.

4.2. Comparison of results on distinct platforms

The proposed test system is also set up and simulated separately in Matlab/Simulink and OpenDSS. Table 2 demonstrates the results of these two test systems, WMC and IEEE-PES data, in terms of maximum/minimum bus voltage magnitude and power losses. Table 2 shows these four distinct platforms' results are pretty close and almost identical.

As shown in Table 2, the maximum voltage magnitude is calculated at 83-bus using the Matlab/Simulink platform. Vmax is determined at 149-bus in other platforms. Voltage values of phase A of 83-bus show 1.0436, 1.0439,10424, and 1.0436 for solvers, respectively. As shown in Fig. 4, the 83-bus and 149-bus (slack bus) locations are not near each other; however, the 83-bus and the slack bus voltage values are pretty close. The reason for this is that a 3-phase capacitor tank (200 kVAr at each-phase) is connected to 83-bus. The calculated voltage values at 149-bus are 1.0437 for phases A, B, and C in the Matlab/Simulink platform (almost the same as other solvers). A slight difference has occurred between Matlab/Simulink and the other platforms because Matlab/Simulink performs the simulation in the time domain.

5. Results and discussion

In this paper, a 123-bus test system is conducted using the SMA algorithm. The study consists of two different scenarios, with further case studies under each. In scenario I, the objective function is the voltage profile enhancement and active power loss minimization. Scenario II involves a different objective function for the test system. The aim is to minimize the VUI and CUI, which are two metrics used to evaluate power distribution system performance, by considering different cases. In the first case, the mean values of VUI and CUI are minimized. In the second case, the highest values of VUI and CUI are reduced. In the third case, the CUI value at the feeder point is decreased using reconfiguration. In literature, it is stated that the VUI is limited to up to 3 % and there is no standard for CUI, but the advised limit is 30 % [20].This CUI approximation is feasible for small-scale such as 19-bus and 25-bus unbalanced test systems; however, it does not present a reasonable solution when a 123-bus test system is considered [24]. For instance, in the original configuration, the maximum value of the CUI at bus-65 is 45.72 %, which is larger than 30 % [21]. The performance of the SMA is also compared statistically with the two popular metaheuristic algorithms, EO and DE. All simulations are run on a computer with an i5-7400 T processor with a speed of 2.40 GHz.

5.1. Scenario I

In this scenario, the objective function is to minimize the power loss in the 123-bus UPDN. The system is examined in four cases to obtain the most power loss reduction. In the literature, the 123-bus RecPrb works have been mainly realized considering case 1 and case 2. In previous studies, the possible reconfiguration number is calculated as 11 and 66 for case-1 and case-2, respectively. In this paper, the complexity is increased by adding 3 more tie-switches into the PDN, and the possible radial configuration number is increased to 677893. Table 3 shows the possible radial configuration number depending on the SSs and TSs.

Table 2
123-bus radial UPDN power flow results for initial case.

	IEEE Test Case	Matlab/ Simulink	OpenDSS	WMC
Tie-Switches	54–94 (Sw 9) 151–300 (Sw 10)	54–94 (Sw 9) 151–300 (Sw 10)	54–94 (Sw 9) 151–300 (Sw 10)	54–94 (Sw 9) 151–300 (Sw 10)
$\mathbf{P_{loss}}$ (kW)	**95.611**	**95.519786**	**95.2828**	**95.59387**
$\mathbf{Q_{loss}}$ (kVAr)	193.727	192.39776	190.9900	192.46491
$\mathbf{S_{loss}}$ (kVA)	216.036	214.80439	213.4385	214.89749
$\mathbf{V_{min}}$ (pu)	0.9856	0.98582	0.98579	0.98585
Bus No, Phase	Bus-65, [A]	Bus-65, [A]	Bus-65, [A]	Bus-65, [A]
$\mathbf{V_{max}}$ (pu)	1.0438	1.0439	1.0437	1.0437
Bus No, Phase	Bus-149, [B], [C]	Bus-83, [A]	Bus-149, [A], [B], [C]	Bus-149, [A], [B], [C]

Table 3
Possible radial configuration number for each case of Scenario I.

	In the literature		In this study	
	In Case-1 [15,19]	In Case-2 [17,19]	In Case-3	In Case-4
SSs Number	12	12	130	133
TSs Number	2	2	2	5
Possible Radial Configurations Number	11(a*)	66(b*)	322 (b*)	**677,893** (b*)

where (a*): switch 9 and the branch between 93 and 94 are given as one phase, and (b*): switch 9 and the branch between 93 and 94 are assumed as three-phase to increase the complexity of PDNR. In case-3 and case-4, the possible radial configuration (feasible combination) number is calculated using the Laplacian matrix technique.

5.1.1. Case-1 for scenario I

In this case, reconfiguration is carried out using IEEE-PES data. Initially, 54–94 and 151–300 switches (9 and 10) were open. After optimization, the 151–300 switch is closed, and the 97–197 switch is opened. The comparison results in terms of power loss and voltage profile are shown in Table 4. While the initial active power loss value is determined as 95.59 kW, it is reduced to 93.87 kW after optimization. Thus, the active power loss is minimized, and the radiality of the system is provided. The minimum bus voltage value is calculated as 0.96p.u at bus-114/phase A.

5.1.2. Case-2 for scenario I

The branch between 93 and 94 was given as a single phase (phase A) in Ref [31]. This branch is modified as a three-phase to increase the search space and complexity. The reconfiguration process is carried out according to *this assumption which is valid for all cases except* scenario I/case-1. After optimization, 60–160 and 97–197 switches are opened, and the active power loss is determined as 89.439 kW. The minimum bus voltage magnitude is computed as 0.966p.u at bus-114/phase A, similar to case-1. The results obtained are demonstrated in Table 5.

5.1.3. Case-3 for scenario I

In case-1 and case-2, two out of 12 switches are chosen during optimization. In this case, it is assumed that switches (130 switches) are placed on each branch. Thus, the search space and the complexity are increased. After the optimization, 67–72 and 151–300 switches are opened, and the active power loss is decreased to 87.753 kW. The minimum voltage value is calculated as 0.98373p.u at bus-65/phase A. Table 6 compares the simulation platforms' results considering power loss and voltage value.

5.1.4. Case-4 for scenario I

In this part, it is assumed that switches are placed on all branches as in case-3. Furthermore, the system is modified by adding 3 TSs, as shown in Table 7. The reasons for adding TSs can be explained as follows: (a) minimizing the affected customer numbers in the case of a fault occurs, (b) increasing the system's complexity to observe the algorithms' performance, (c) minimizing the active power loss.

The results obtained are shown in Table 8. The active power loss is decreased to 83.592 kW after reconfiguration. The minimum voltage magnitude is determined as 0.988p.u at bus-63/phase A. Compared to the initial case, more power loss reduction is provided in case-4.

Comparing the four cases can be concluded that the active power loss decreases further in each case from case-1 to case-4, respectively. Even in the worst case, the minimum voltage of the buses remains above 0.95p.u (without changing the initial voltage regulator tap settings).

5.2. Performance of the algorithms

In this study, the performance of the algorithms is compared considering system design in case-4 (where TSs are added to the system). In this section, the performances of SMA, DE, and EO metaheuristic search algorithms are tested in solving the RecPrb by considering more than 15 statistical data.

5.2.1. Comparison of tested algorithms

The objective function aims to enhance the bus voltage magnitude and decrease power losses. In Table 9, the active power losses in the best/worst and average cases are compared. All tested algorithms are run 500 times independently. The algorithms' population size and maximum iteration are chosen as 100 and 200, respectively. The algorithms sometimes get caught up in local minima and thus cannot detect the global point. It is noticed that the SMA (152) reaches the global minimum point successfully with the highest number, and it is followed up with EO (75 times) and DE (4 times).

The DE algorithm gets stuck in local minima at most. The SMA and EO are the closest algorithms to the global optima, even in the worst switching position case. The average power loss value is almost the same for the three algorithms. In this respect, all three algorithms perform well in solving the RecPrb.

5.2.2. Statistical evaluation of algorithms

In this work, the 123-bus UPDN reconfiguration problem is examined comprehensively and in detail. The SMA, EO, and DE algorithms are evaluated using various statistical methods to find the best technique which solves RecPrb in a UPDN test system. The performances of the algorithms are evaluated considering many statistical methods presented in Table 10, such as mode, median, relative error (RE), mean squared error (MSE), standard deviation (STD), root mean square error (RMSE), mean absolute error (MAE), standard error (SE).

These statistical parameters let us evaluate all algorithms under the same test conditions. As seen in Table 10, considering all the statistical data, SMA shows the best performance, and DE shows the poorest performance. Results are overall based on the mean values because they are calculated using error formulas that do not give much information regarding reaching the global optima. Analyzing Table 9 and Table 10, the SMA algorithm offers the best result since its number of finding the

Table 4
123-bus UPDN power flow results after reconfiguration for the scenario I/case-1.

	Matlab/ Simulink	OpenDSS	WMC
Tie-Switches	54–94 (Sw 9) 97–197 (Sw 5)	54–94 (Sw 9) 97–197 (Sw 5)	54–94 (Sw 9) 97–197 (Sw 5)
$\mathbf{P_{loss}}$(kW)	**93.79382**	**93.9901**	**93.879013**
$\mathbf{Q_{loss}}$(kVAr)	188.51689	188.04100	188.61745
$\mathbf{S_{loss}}$ (kVA)	210.56092	210.22635	210.68890
$\mathbf{V_{min}}$(pu)	0.96673	0.96014	0.966699
Bus No, Phase	Bus-114,[A]	Bus-114,[A]	Bus-114,[A]
$\mathbf{V_{max}}$(pu)	1.0531	1.0446	1.0531
Bus No, Phase	Bus-83,[A]	Bus-83,[A]	Bus-83,[A]

Table 5
123-bus UPDN power flow results after reconfiguration for the scenario I/case-2.

	Matlab/ Simulink	OpenDSS	WMC
Tie-Switches	60–160 (Sw 3) 97–197 (Sw 5)	60–160 (Sw 3) 97–197 (Sw 5)	60–160 (Sw 3) 97–197 (Sw 5)
$\mathbf{P_{loss}}$ (kW)	**89.49462**	**89.0891**	**89.43945**
$\mathbf{Q_{loss}}$ (kVAr)	179.509420	177.954	179.54766
$\mathbf{S_{loss}}$ (kVA)	200.581456	199.008778	200.59108
$\mathbf{V_{min}}$ (pu)	0.96602	0.96598	0.966001
Bus No, Phase	Bus-114,[A]	Bus-114,[A]	Bus-114,[A]
$\mathbf{V_{max}}$ (pu)	1.0437	1.0437	1.0437
Bus No, Phase	Bus-149,[A], [B], [C]	Bus-149,[A], [B], [C]	Bus-149,[A], [B], [C]

Table 6
123-bus UPDN power flow results after reconfiguration for the scenario I/case-3.

	Matlab/ Simulink	OpenDSS	WMC
Tie-Switches	67–72 (Branch) 151–300 (Sw10)	67–72 (Branch) 151–300 (Sw10)	67–72 (Branch) 151–300 (Sw10)
$\mathbf{P_{loss}}$ (kW)	**87.76797**	**87.4053**	**87.75328**
$\mathbf{Q_{loss}}$ (kVAr)	176.78772	175.273	176.78189
$\mathbf{S_{loss}}$ (kVA)	197.37556	195.85788	197.36381
$\mathbf{V_{min}}$ (pu)	0.98377	0.98373	0.98372
Bus No, Phase	Bus-65,[A]	Bus-65,[A]	Bus-65,[A]
$\mathbf{V_{max}}$ (pu)	1.0437	1.0437	1.0437
Bus No, Phase	Bus-149,[A], [B], [C]	Bus-149,[A], [B], [C]	Bus-149,[A], [B], [C]

Table 7
Additional tie-switches' location and length.

Tie-Switch No	From Bus	To Bus	Length (Feet)	Line Configuration No
3	35	66	750	12 (3 ~ underground line)
4	83	195	1500	2 (3 ~ overhead line)
5	251	300	2000	1 (3 ~ overhead line)

Table 8
123-bus UPDN power flow results after reconfiguration for the scenario I/case-4.

	Matlab Simulink	OpenDSS	WMC
Tie-Switches	47–49, 64–65, 72–76, 76–77, 108–300	47–49, 64–65, 72–76, 76–77, 108–300	47–49, 64–65, 72–76, 76–77, 108–300
$\mathbf{P_{loss}}$ (kW)	**83.661686**	**83.6061**	**83.592732**
$\mathbf{Q_{loss}}$ (kVAr)	169.04662	168.146	169.16238
$\mathbf{S_{loss}}$ (kVA)	188.61611	187.78460	188.68931
$\mathbf{V_{min}}$ (pu)	0.98832	0.9883	0.988303
Bus No, Phase	Bus-63, [A]	Bus-63, [A]	Bus-63, [A]
$\mathbf{V_{max}}$ (pu)	1.0437	1.0437	1.0437
Bus No, Phases	Bus-149, [A], [B], [C]	Bus-149, [A], [B], [C]	Bus-149, [A], [B], [C]

global minima with a high success rate and has the best statistical values. Table 11 shows the tested algorithms' converge characteristics to catch global or local minima points.

SMA has reached the global/local minima point on average iteration with 117.88 out of 200. In this respect, SMA shows the best converge (performance) characteristic. In addition, the DE algorithm shows the worst performance with 141.71 iterations. Converge characteristic does not provide adequate information about the algorithm performances. Therefore, it should be considered with other parameters to make a proper evaluation. Table 12 demonstrates the algorithms' elapsed times to complete the loop regarding median, maximum, minimum, and average time. Elapsed times changes based on algorithm performances, problem types, and computer hardware configuration. DE demonstrates the best performance in all situations except minimum time.

The graphical representation of the statistical values obtained in Table 12 is shown in Fig. 8.

5.3. Scenario II

The aim of this scenario is the minimization of unbalanced indexes by considering them as an objective function. The unbalance index formula is given in Eq. (16). In this section, the data and conditions of *scenario I/case-3* are used for the study to be reproducible and to increase the complexity of the calculations. Different cases are considered to minimize the CUI and VUI in the 123-bus UPDN.

Table 9
Active power losses in best and worst cases and their switch positions.

Algorithm Name	Best Case $\mathbf{P_{loss}^{min}}$ (**kW**)	Worst Case $\mathbf{P_{loss}^{max}}$ (**kW**)	Average $\mathbf{P_{loss}^{Ave}}$ (**kW**)	No of Global Optima out of 500 Times	**OpenSwitches** (Tie-Switches) for Best Case	**OpenSwitches** (Tie-Switches) for Worst Case	% Power Loss Reduction for $\mathbf{P_{Loss}^{Best}}$&$\mathbf{P_{Loss}^{Worst}}$
DE	**83.592732**	84.554	83.898	4 / 500	47–49, 64–65, 72–76 76-77, 108-300	60–62, 72–76,76–77, 250-251, 151-300	12.554 % (Best) 11.549 % (Worst)
EO	**83.592732**	84.250	83.774	75 / 500	47–49. 64–65, 72–76 76-77, 108-300	29–30, 50–51, 64–65, 67–72, 76–77	12.554 % (Best) 11.867 % (Worst)
SMA	**83.592732**	84.250	83.709	152 / 500	47–49. 64–65, 72–76 76-77, 108-300	29–30, 50–51, 64–65, 67–72, 76–77	12.554 % (Best) 11.867 % (Worst)

Table 10
Algorithm's statistical evaluations.

Algorm. Name	STD (σ)	Stand Error	MSE	RMSE	%RE	MAE	Median	Mode	Variance
DE	0.18396	0.0082269	0.12689	0.35622	0.36371	0.30515	83.772	83.731	0.033841
EO	0.14684	0.0065734	0.054488	0.23343	0.21674	0.18158	83.730	83.730	0.021562
SMA	0.11773	0.0030687	0.027267	0.16513	0.13836	0.11582	83.730	83.730	0.013861

Table 11
Converge characteristics of search algorithms.

Algorithms Name	Number of Iterations for $\mathbf{P}_{\mathbf{loss}}^{\mathbf{min}}(\mathbf{kW})$		
	Maximum	Minimum	Average
DE	200	9	141.71
EO	200	15	123.89
SMA	182	42	117.88

In the first case, the mean values of the CUI and VUI for the entire system; in the second case, the maximum values of the CUI and VUI; and in the third case, the CUI value at the feeder point are minimized using the reconfiguration process. The VUI is limited to up to 3 %, and there is no standard for CUI, but the advised limit is 30 %.The CUI approximation has been found to be a viable method for smaller-scale power systems, specifically those with 19-bus and 25-bus unbalanced configurations, as noted in Ref. [24]. However, its efficacy diminishes when applied to larger systems such as the 123-bus test systems, where it fails to produce solutions deemed reasonable by prevailing standards. For instance, in the original configuration, the maximum value of the CUI at bus-65 is 45.72 %, which is larger than 30 %. In this study, the mean value of the CUI decreased from 13.34 % to 10 % after the reconfiguration approach.

5.3.1. CUI optimization

In this section, three cases are studied to minimize the CUI value. The calculation formula of CUI is given in Eq. (16). To calculate the CUI value of any bus, A, B, and C phases should have a non-zero value. CUI cannot be calculated if any of these values are equal to zero. The IEEE-PES solution neglects the currents in m/μ Amper levels and assumes zero at any buses. On the other hand, the OpenDSS simulation platform does not accept the current value as zero at any buses. Thus, in this work, the IEEE-PES approach is used as a reference to calculate CUI. Figs. 9 and 10 demonstrate the CUI results of IEEE-PES and OpenDSS approaches, respectively.

After neglecting leakage currents, the buses that exceed the 30 % CUI limit are as follows in sequence: **65** (45.72 %), **86** (37.31 %), **87** (31.98 %), **91** (44.72 %).

For instance, IEEE data and OpenDSS results for the 30th and 56th buses are given in Table 13. At the 30th bus, the current values of the IEEE data and OpenDSS program are calculated as 0 and 0.68 mA for phase A and 0 and 0.59 mA for phase B, respectively. CUI value calculation is not applicable according to the IEEE-PES approach. However, the OpenDSS program calculates the CUI value as 100.01 % due to leakage currents.

As seen in Fig. 9 (leakage currents are neglected), the CUI value exceeding the 30 % limit is available in four buses. Fig. 10 demonstrates the calculated CUI values based on the OpenDSS approach. There are 20 CUI values exceeding the 30 % limit. Therefore, in this study, calculations are carried out considering the IEEE-PES assumption.

Non-neglecting leakage currents, the buses that exceed the 30 % CUI limit are as follows in sequence:**23** (50.96 %), **25** (53.88 %), **28** (58.47 %), **29** (50.96 %), **30** (100.01 %), **50** (58.08 %), **51** (100.03 %), **55** (49.192 %), **56** (100.01 %), **65** (45.72 %), **66** (100.02 %), **79** (100 %), **86** (37.31 %), **87** (31.98 %), **91** (44.72 %), **93** (49.07 %), **95** (100 %), **99** (50.26 %), **100** (100.02 %), **105** (54.55 %), **108** (100.01 %).

5.3.1.1. Case-1 for CUI optimization. In this case, the objective function is to minimize the mean of the CUI value by considering the current flow in all branches of the test system. After the reconfiguration process, the results are as follows: The switches 53–54 and 67–72 are opened. Thus, the radiality of the network is maintained. The mean value of CUI was initially calculated as **13.34** and decreased to **10.009**. The minimum bus voltage magnitude is calculated as 0.9232 at bus-71/phase A. The active power loss was initially **95.59** kW and has increased to **178.5259** kW. Therefore, a conflict has occurred between the mean CUI value and the active power loss. The decision-maker should consider this conflict in terms of the PDN operation requirements. The bus-65 is the only one that exceeds the 30 % CUI limit and is calculated as 47.11 %. The rest of the busses' CUI values has remained under 30 %. The results are shown in the case-1 column of Table 14.

5.3.1.2. Case-2 for CUI optimization. In this case, the objective function is to minimize the maximum value of CUI in the test system. After the

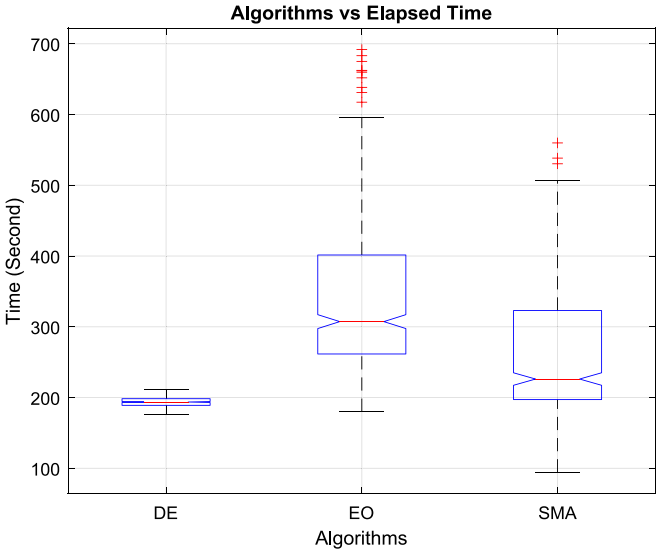

Fig. 8. Elapsed times.

Table 12
Comparison of algorithms considering the elapsed time.

Algorithms Name	Elapsed Time (seconds)						
	Maximum	Minimum	Average	Median	Upper Adjacent	Lower Adjacent	Outliers No
DE	211.7407	175.3946	193.8	193.69	211.7407	175.3946	0
EO	691.8054	179.9317	339.14	307.33	595.6451	179.9317	10
SMA	559.8522	94.2545	254.54	226.16	506.4191	94.2545	3

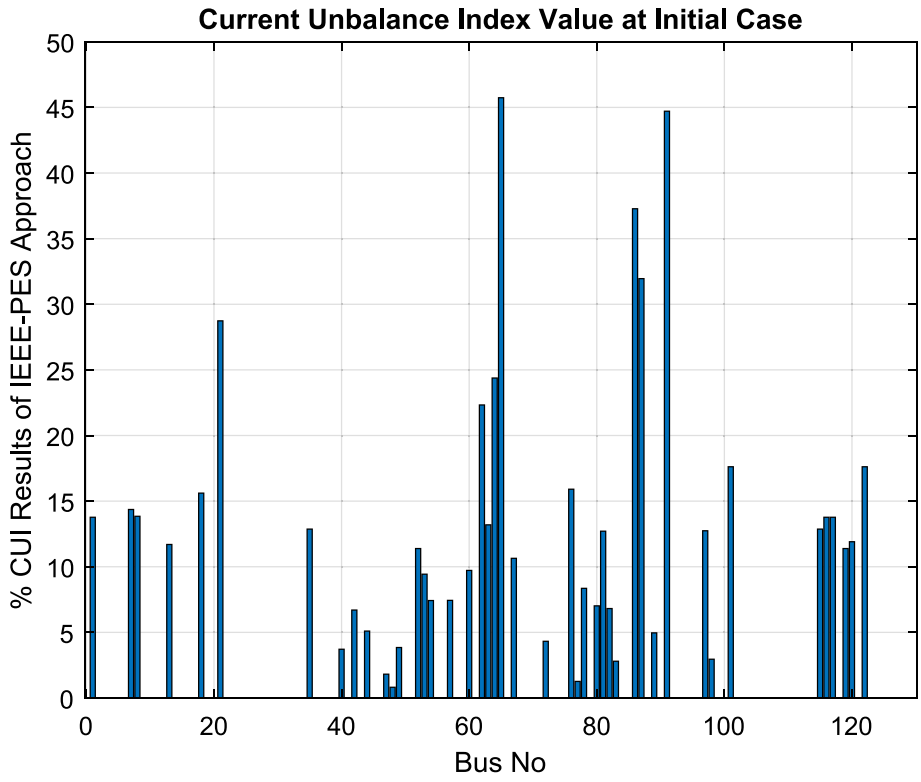

Fig. 9. Neglected leakage current in the power network.

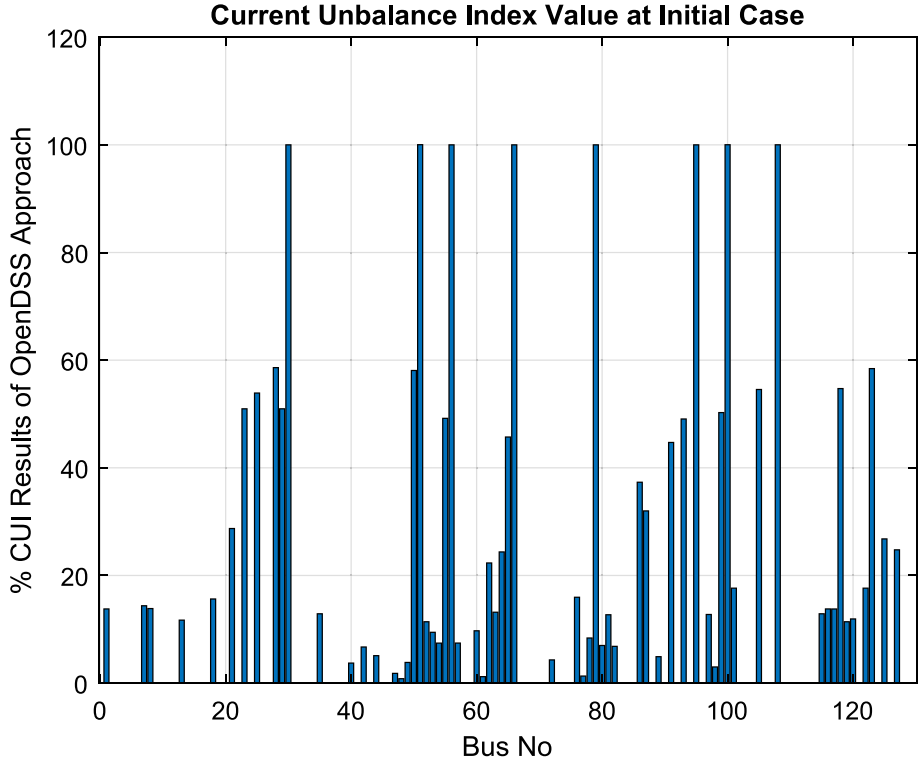

Fig. 10. Non-neglecting leakage currents in the power network.

reconfiguration process, the results are as follows: The switches 57–60 and 105–108 are opened. Thus, the radiality of the network is maintained. The highest CUI value was initially 45.718 at bus-65 and decreased to 45.305. The minimum bus voltage magnitude is calculated as 0.96 at bus-114/phase A. The active power loss was initially **95.59** kW and increased to **100.755** kW. The bus-49, bus-65, and bus-97 have exceeded the 30 % CUI limit with values of 38.49 %, 45.30 %, and 31.32 %, respectively. The rest of the busses' CUI values remain under 30 %.

Table 13
IEEE-PES and OpenDSS current calculations approach.

	Bus No	Current Phase [A]	Current Phase [B]	Current Phase [C]	CUI Value
IEEE-PES [31]	30	0.00	0.00	18.470 A	N. A
	56	0.00	9.01 A	0.00	N. A
OpenDSS	30	0.68 mA	0.59 mA	18.437 A	100.01
	56	2.03e-12	9.0102 A	1.5e-11	100.01

The mean CUI value in the power network has increased from 13.34 to 15.09. On the other hand, the CUI on the feeder bus (bus-149) has decreased from **13.76** to **13.37**. The results are shown in the case-2 column of Table 14.

5.3.1.3. Case-3 for CUI optimization. In this case, the objective function is to minimize the CUI at the feeder bus. After the reconfiguration process, the results are as follows: The switches 54–57 and 105–108 are opened. Thus, the radiality of the network is maintained. The CUI at the feeder bus has decreased from 13.766 to 13.358. The active power loss was initially **95.59** kW and increased to **101.557** kW. The highest CUI value was initially 45.718 at bus-65 and decreased to 45.305.

The mean value of CUI has increased from 13.34 to 14.26. The minimum bus voltage magnitude is calculated as 0.96 at bus-114/phase A. The bus-49, bus-65, and bus-97 have exceeded the 30 % CUI limit with values of 38.49 %, 45.31 %, and 31.13 %, respectively. The rest of the busses' CUI values has remained under 30 %. The results are demonstrated in the case-3 column of Table 14. The identical switch configuration in scenario I/case-3 is used and presented in Table 14. The obtained CUI results depend on these TSs are demonstrated in the 4th column from the end.

5.3.2. VUI optimization

Two cases are studied in this subsection, considering the VUI value minimization. The calculation formula of VUI is given in Eq. (16). There are different standards to limit voltage unbalanced index. The American National Standard for Electric Power Systems and Equipment ANSI C84.1 states that the voltage unbalance limit should be up to 3 %, and the NEMA defines the VUI limit as 1 % [20].

5.3.2.1. Case-1 for VUI optimization. In this case, the objective function is to minimize the mean of VUI by considering voltage magnitudes in all branches of the test system. After the reconfiguration process, the results are as follows: The switches 86–87 and 101–105 are opened. Thus, the network maintains its radiality. The mean value of VUI, which was 0.867 initially, has decreased to 0.759. The active power loss has decreased to **91.334** kW. The minimum bus voltage magnitude is calculated as 0.959 at bus-114/phase A. The VUI of bus-108 is calculated as 1.13 %, which is the highest index value. Initially, the total 19 busses as 60,61,62,63,64,65, 86,87,89,91,93,95, 105,108, 160, 195, 300, 350, 610 exceed the 1 % VUI limit. After the reconfiguration, the number of busses (51,105,108, 151, 300, 350), which exceed the 1 % VUI limit, has decreased to 6 in total. The results are shown in the case-1 column of Table 15.

5.3.2.2. Case-2 for VUI optimization. In this case, the objective function is to minimize the VUI's maximum value in the test system. After the reconfiguration process, the results are as follows: The switches 89–91 and 108–300 are opened. The highest VUI value was initially 1.078 at bus-95 and bus-195 and has decreased to 1.008 at bus-60 and bus-160.

The active power loss has reduced to 93.144 kW. The minimum bus voltage magnitude is calculated as 0.98 at the bus-65/phase A. Bus-60, bus-61, bus-160, and bus-610 have exceeded the 1 % VUI limit. The rest of the buses' VUI values remain under 1 %. The mean VUI value has decreased from 0.867 to 0.829. On the other hand, the VUI on the feeder bus (bus-149) does not change with the reconfiguration process. In case-2 column of Table 15 shows VUI results after reconfiguration. The identical switch configuration based on the scenario I/case-3 is used and presented in Table 15. The obtained VUI results based on these TSs are demonstrated in the 3rd column from the end.

5.4. Summary of results and discussion

In summary, the study consists of two different scenarios, and there are further case studies under each scenario. In the scenario I, the objective function is the voltage profile enhancement and active power loss minimization. In scenario II, another objective function is defined for the test system as minimizing the VUI and CUI by considering different cases for each.

Scenario I consists of four distinct cases, as summarized in Table 3. In Case 1 and Case 2, the reconfiguration is carried out by selecting only two out of the twelve switches provided by IEEE. These cases are a repetition or reapplication of previous studies found in the literature. In Case 3 and Case 4, unlike the literature, the number of switches is

Table 14
Current unbalance index (CUI) results after reconfiguration.

			Case-1	Case-2	Case-3
	Initial Case	Power Loss as an objective function	Mean of CUI in PDN	Min. of Highest CUI value in PDN	Min. of CUI at Feeder Bus (149)
Tie-Switches	54–94, 151–300	67–72 151–300	53–54 67–72	57–60 105–108	54–57 105–108
Feeder Bus CUI value (at Bus-149)	**13.7661138**	13.5942927	13.7224301	13.3775645	**13.3588277**
Mean of CUI value	**13.3451517**	12.9208084	**10.0094624**	15.0959342	14.2679555
Max. CUI value	**45.7187944**	45.65196178	47.1116728	**45.3058710**	45.307953
Bus No	**Bus-65**	Bus-65	Bus-65	**Bus-65**	Bus-65
Minimum Voltage	0.9858562,	0.983762319,	0.923227427,	0.960118	0.96015280
Bus No,	Bus-65,	Bus-65,	Bus-71,	Bus-114,	Bus-114,
Phase	[A]	[A]	[A]	[A]	[A]
Maximum Voltage	1.04375	1.04375	1.04375	1.04375	1.04375
Bus No,	Bus-149	Bus-149	Bus-149	Bus-149	Bus-149
Phase	[A], [B], [C]	[A], [B], [C]	[A], [B], [C]	[A], [B], [C]	[A], [B], [C]
Active [kW] &	**95.593872**	**87.70667**	178.5259589	100.7559766	101.55728441
Reactive [kVAr] Power Loss	j192.464919	j176.68291	j361.42980657	j199.8040703	j201.4586534
Bus Number of over the 30 % CUI value	65 (45.72 %), 86 (37,31 %), 87 (31.98 %), 91 (44.72 %)	65 (45.65 %), 160 (32.01 %)	65 (47.11 %)	49 (38.49 %), 65 (45.30 %), 97 (31.32 %)	49 (38.49 %), 65 (45.31 %), 97 (31.13 %)

Table 15
Voltage unbalance index (VUI) results after reconfiguration.

			Case-1	Case-2
	Initial Case	Power Loss as an objective function	Mean of VUI in PDN	Min. of highest VUI value in PDN
Tie-Switches	54–94, 151–300	67–72 151–300	86–87, 101–105	89–91, 108–300
Feeder Bus VUI value (at Bus 149)	1.5857e-14	1.5857e-14	1.5857e-14	1.5857e-14
Mean of VUI value	**0.867437048**	0.8359582626	**0.7595776406**	0.8298028354
Maximum VUI value Bus No	**1.0780543644** **Bus-95, and** **Bus-195**	1.1109174656 Bus-60, and Bus-160	1.1340169787 Bus-108	**1.0086615616** **Bus-60, and** **Bus-160**
Minimum Voltage Bus No, Phase	0.9858562, Bus-65, [A]	0.983762319, Bus-65, [A]	0.9598660304 Bus-114 [A]	0.987034481 Bus-65 [A]
Maximum Voltage Bus No, Phase	1.04375 Bus-149 [A], [B], [C]	1.04375 Bus-149 [A], [B], [C]	1.0593924620 Bus-83 [A]	1.0458859587 Bus-83 [A]
Active [kW] & Reactive [kVAr] Power Loss	**95.593872** j192.464919	**87.70667** j176.68291	91.3348699 j183.5865456	93.14440336 j187.38053853
Bus Number of over the % 1 VUI value	60,61,62,63,64,65, 86,87,89,91,93,95, 105,108,160,195,300,350,610	60,61,62,63,64, 65,66,160,610	51,105,108,151,300,350	60, 61, 160, 610

increased. In Case 3, it is assumed that there are 130 SSs in total, assuming that there is a switch between every two buses, which increase the total number of possible radial configurations to 322. In order to ensure the radiality of the PDN, 2 TSs are opened as a result of reconfiguration process. In Case 4, an extra 3 TSs are added to the PDN (5 TSs in total), the number of SSs is increased to 133 and the number of possible radial configurations increases to 677893. The aim here is to test the performance of the search algorithm by expanding the search space of the system, reduce the active power loss of the PDN and improve the voltage profile.

The active power loss (for initial case) is 95.59 kW, reduced to 93.87 kW in case 1, 89.44 kW in case 2, 87.75 kW in case 3, and 83.59 kW in case 4. As a result, total active power loss is reduced up to 12.55 %.

Scenario II consists of three cases for the enhancement of the CUI and two cases for the improvement of the VUI. The results of these cases are presented in Table 14 and Table 15. In the first case, the mean values of the VUI and CUI; in the second case, the maximum values of the VUI and CUI; and in the third case, the CUI value at the feeder point are minimized using reconfiguration method. In previous studies it is stated that the VUI is limited to up to 3 %, and there is no standard for CUI, but the advised limit is 30 %. This CUI approximation is feasible for small-scale such as 19-bus and 25-bus unbalanced test systems; however, it does not present a reasonable solution when a large-scale 123-bus test system is considered. For instance, in the original configuration, the maximum value of the CUI at bus-65 is 45.72 %, which is larger than 30 %.

6. Conclusion

In this paper, a slime mould algorithm is used to solve the reconfiguration problem based on 123-bus UPDN. The objective function of this method is the minimization of power loss, VUI, and CUI values. RecPrb in PDN has conventionally been approached as single-phase balanced modeling. The presented method approaches the problem by considering real unbalanced test systems. Unbalanced indexes are critical power quality problems that are highly harmful to PDN. Thus, unbalanced indexes have been examined in detail separately, considering many cases to demonstrate their effects in a UPDN test system. In all presented cases, when the voltage unbalanced index is regarded as an objective function, VUI and power loss decrease after the reconfiguration process compared to the initial case. Considering the current unbalanced index as an objective function leads to a reduction in CUI and an increment in power loss after reconfiguration. Based on the results obtained, it can be concluded that minimizing the VUI is proportional to power loss reduction. On the other hand, CUI optimization has an inverse effect on power loss which increases with CUI decrement. A Matlab script is written, and all simulations are executed in the Matlab environment. The correctness and the success of the results obtained from WMC are validated by setting up the test system in OpenDSS and Matlab/Simulink and making a comparison with the results of these platforms. The SMA technique is compared with the popular EO and DE algorithms by using more than 15 statistical methods to show the technique's efficiency in solving unbalanced test system reconfiguration problems. The SMA is an efficient and robust method for minimizing power losses, limiting unbalanced indexes, and enhancing the system's voltage profile.

CRediT authorship contribution statement

Nisa Nacar Cikan: Conceptualization, Data curation, Formal analysis, Investigation, Methodology, Software, Validation, Writing – original draft, Writing – review & editing. **Murat Cikan:** Data curation, Software, Validation, Writing – review & editing.

Declaration of competing interest

The authors declare that they have no known competing financial interests or personal relationships that could have appeared to influence the work reported in this paper.

Data availability

Data will be made available on request.

References

[1] Wang J-C, Chiang H-D, Darling GR. An efficient algorithm for real-time network reconfiguration in large scale unbalanced distribution systems. IEEE Trans Power Syst 1996;11(1):511–7. https://doi.org/10.1109/59.486141.
[2] Sultana B, Mustafa MW, Sultana U, Bhatti AR. Review on reliability improvement and power loss reduction in distribution system via network reconfiguration. Renew Sustain Energy Rev 2016;66:297–310. https://doi.org/10.1016/j.rser.2016.08.011.
[3] Cikan M, Kekezoglu B. Comparison of metaheuristic optimization techniques including Equilibrium optimizer algorithm in power distribution network reconfiguration. Alexandria Eng J 2022;61(2):991–1031. https://doi.org/10.1016/j.aej.2021.06.079.
[4] Radosavljević J. Metaheuristic optimization in power engineering. Inst Eng Technol 2018.
[5] Mishra S, Das D, Paul S. A comprehensive review on power distribution network reconfiguration. Energy Syst 2017;8(2):227–84. https://doi.org/10.1007/s12667-016-0195-7.

[6] F. Yang and Z. Li, "Effects of balanced and unbalanced distribution system modeling on power flow analysis," in 2016 IEEE Power & Energy Society Innovative Smart Grid Technologies Conference (ISGT), 2016, pp. 1–5, doi: 10.1109/ISGT.2016.7781195.
[7] Wang H-J, Pan J-S, Nguyen T-T, Weng S. Distribution network reconfiguration with distributed generation based on parallel slime mould algorithm. Energy 2022;244:123011. https://doi.org/10.1016/j.energy.2021.123011.
[8] S. Heang, V. Vai, P. Hem, D. Eam, L. You, and S. Eng, "Optimal Network Reconfiguration with DGs Placement and Sizing in a Distribution System Using Hybrid SOE and GA," in 2022 19th International Conference on Electrical Engineering/Electronics, Computer, Telecommunications and Information Technology (ECTI-CON), 2022, pp. 1–4, doi: 10.1109/ECTI-CON54298.2022.9795530.
[9] M. M. Sayed, M. Y. Mahdy, S. H. E. A. Aleem, H. K. M. Youssef, and T. A. Boghdady, "Simultaneous Distribution Network Reconfiguration and Optimal Allocation of Renewable-Based Distributed Generators and Shunt Capacitors under Uncertain Conditions," Energies, vol. 15, no. 6, 2022, doi: 10.3390/en15062299.
[10] Naderipour A, Abdullah A, Marzbali MH, Arabi Nowdeh S. An improved corona-virus herd immunity optimizer algorithm for network reconfiguration based on fuzzy multi-criteria approach. Expert Syst Appl 2022;187:115914. https://doi.org/10.1016/j.eswa.2021.115914.
[11] Zhai HF, Yang M, Chen B, Kang N. Dynamic reconfiguration of three-phase unbalanced distribution networks. Int J Electr Power Energy Syst 2018;99:1–10. https://doi.org/10.1016/j.ijepes.2017.12.027.
[12] Kaur M, Ghosh S. Network reconfiguration of unbalanced distribution networks using fuzzy-firefly algorithm. Appl Soft Comput 2016;49:868–86. https://doi.org/10.1016/j.asoc.2016.09.019.
[13] R. A. Jacob, S. Paul, W. Li, S. Chowdhury, Y. R. Gel, and J. Zhang, "Reconfiguring Unbalanced Distribution Networks using Reinforcement Learning over Graphs," in 2022 IEEE Texas Power and Energy Conference (TPEC), 2022, pp. 1–6, doi: 10.1109/TPEC54980.2022.9750805.
[14] Zheng W, Huang W, Hill DJ. A deep learning-based general robust method for network reconfiguration in three-phase unbalanced active distribution networks. Int J Electr Power Energy Syst 2020;120:105982. https://doi.org/10.1016/j.ijepes.2020.105982.
[15] P. Gangwar, S. N. Singh, and S. Chakrabarti, "Network reconfiguration for unbalanced distribution systems," in TENCON 2017 - 2017 IEEE Region 10 Conference, 2017, pp. 3028–3032, doi: 10.1109/TENCON.2017.8228381.
[16] M. Quintero-Duran, J. Candelo-Becerra, and J. Soto Ortiz, "A modified backward/forward sweep-based method for reconfiguration of unbalanced distribution networks," Int. J. Electr. Comput. Eng., vol. 9, pp. 85–101, Feb. 2019, doi: 10.11591/ijece.v9i1.pp.85-101.
[17] Gerez C, Costa ECM, Sguarezi Filho AJ. Static reconfiguration of unbalanced distribution systems with variable power using selective bat algorithm. J Control Autom Electr Syst 2021;32(3):656–71. https://doi.org/10.1007/s40313-021-00695-z.
[18] Zhou A, Zhai H, Yang M, Lin Y. Three-phase unbalanced distribution network dynamic reconfiguration: A distributionally robust approach. IEEE Trans Smart Grid 2022;13(3):2063–74. https://doi.org/10.1109/TSG.2021.3139763.
[19] Amanulla B, Chakrabarti S, Singh SN. Reconfiguration of power distribution systems considering reliability and power loss. IEEE Trans Power Deliv 2012;27(2):918–26. https://doi.org/10.1109/TPWRD.2011.2179950.
[20] Arghavani H, Peyravi M. Unbalanced current-based tariff. CIRED - Open Access Proc J 2017;2017(1):883–7. https://doi.org/10.1049/oap-cired.2017.0129.
[21] Beneteli TAP, Cota LP, Euzébio TAM. Limiting current and voltage unbalances in distribution systems: A metaheuristic-based decision support system. Int J Electr Power Energy Syst 2022;135:107538. https://doi.org/10.1016/j.ijepes.2021.107538.
[22] "Definitions of Voltage Unbalance," IEEE Power Eng. Rev., vol. 21, no. 5, pp. 49–51, 2001, doi: 10.1109/MPER.2001.4311362.
[23] Cikan M, Cikan NN. Optimum allocation of multiple type and number of DG units based on IEEE 123-bus unbalanced multi-phase power distribution system. Int J Electr Power Energy Syst 2023;144:108564. https://doi.org/10.1016/j.ijepes.2022.108564.
[24] C. Gerez, E. Coelho Marques Costa, and A. J. Sguarezi Filho, "Distribution Network Reconfiguration Considering Voltage and Current Unbalance Indexes and Variable Demand Solved through a Selective Bio-Inspired Metaheuristic," Energies, vol. 15, no. 5, 2022, doi: 10.3390/en15051686.
[25] Li S, Chen H, Wang M, Heidari AA, Mirjalili S. Slime mould algorithm: A new method for stochastic optimization. Futur Gener Comput Syst 2020;111:300–23. https://doi.org/10.1016/j.future.2020.03.055.
[26] Faramarzi A, Heidarinejad M, Stephens B, Mirjalili S. Equilibrium optimizer: A novel optimization algorithm. Knowledge-Based Syst 2020;191:105190. https://doi.org/10.1016/j.knosys.2019.105190.
[27] Storn R, Price K. Differential evolution – A simple and efficient heuristic for global optimization over continuous spaces. J Glob Optim 1997;11(4):341–59. https://doi.org/10.1023/A:1008202821328.
[28] Rajaram R, Sathish Kumar K, Rajasekar N. Power system reconfiguration in a radial distribution network for reducing losses and to improve voltage profile using modified plant growth simulation algorithm with Distributed Generation (DG). Energy Rep 2015;1:116–22. https://doi.org/10.1016/j.egyr.2015.03.002.
[29] R. B. Bapat, "Graphs and Matrices,", 2nd ed., Springer, London, 2014, pp. 13-26.
[30] Ahmadi H, Martí JR. Mathematical representation of radiality constraint in distribution system reconfiguration problem. Int J Electr Power Energy Syst 2015;64:293–9. https://doi.org/10.1016/j.ijepes.2014.06.076.
[31] IEEE PES Distribution Systems Analysis Subcommittee Radial Test Feeders [Online], Available: https://cmte.ieee.org/pes-testfeeders/resources/ (accessed May. 15, 2023).